Power Estimation in Three-Phase PWM Rectifiers Using ANN

Abinash Rath[1], **Satyanarayan Padhy**[2†], **Ankireddy Narendra**[3], **Ashutosh Biswal**[4], and **Kanhu Charan Bhuyan**[5], Non-members

ABSTRACT

At the industrial consumer level, an unbalanced three-phase supply is very common, which creates control issues with PWM rectifiers. Direct power control (DPC) has been a proven controller in the field of rectifier control. The DPC requires the estimation of active and reactive as these quantities are used as the control variable in the loop. For an unbalanced grid, the power estimation becomes complex with the extended *pq* theory. This article presents a novel approach to estimating the instantaneous power using an artificial neural network (ANN), streamlining the complex control structures involving back-to-back connected second-order generalized integrator (SOGI) blocks. The intricate interconnection of multiple SOGI blocks poses challenges in terms of computational complexity. The proposed method leverages ANN to replace the SOGI blocks, which makes the system simpler and more efficient. Rigorous simulation using MATLAB Simulink and comparative studies reveal that with ANN, the performance of the based system can be replicated, and a reduced computational burden can be achieved, leading to improved real-time response. Real-time simulation in RT-LAB validates the proposed ANN-based method for PWM rectifiers' power estimation. Integrating ANN models ensures accurate emulation of complex control structures, affirming the approach's efficacy for industrial deployment.

Keywords: PWM Rectifier, DPC, Artificial Neural Network (ANN), Unbalanced Grid

1. INTRODUCTION

The contemporary power system extensively employs AC to DC converters across various domains, including microgrids, electric vehicle (EV) charging, harnessing energy from renewable sources, active filter controlling, and dual active bridge systems. Specialized tools, actuators, adjustable speed drives, and auxiliary power supply units necessitate rectification within industries. The evolution of AC to DC converters has transitioned from uncontrolled rectifier circuits to PWM rectifiers. The rectifiers have been regulated with great accuracy using diverse control techniques. Among them, direct power control surpasses other approaches as it offers distinct advantages over the rest of the group, such as precise DC voltage control, nearly unity power factor, and enhanced grid power quality [1], [2].

MPC is a prominent controller within the domain of PWM rectifier control because of its numerous advantages [3]–[6]. Various modifications have been made to the cost function to feature multiple extra advantages to the controller. These modifications include minimizing DC link voltage ripple, switching losses, etc. [7].

The introduction of multiple switching vector control with MPC offers a means to diminish deviations in control variables further, potentially utilizing more than one switching vector within a single control period [4], [8]. Research literature highlights numerous efforts to mitigate the computational complexity, a longstanding impediment of MPC. Conversely, it is noted that low-complexity MPC systems may struggle to accommodate additional constraints within the cost function [9], [10]. The literature [10] and [11] also report the deployment of ANN to replace the classical MPC in order to reduce computational complexity. In addition to MPC, the ANN model has also been used to replace different complex controllers [13].

Extended PQ theory is crucial in scenarios where the grid has unbalanced and/or distorted three-phase voltage, as it produces a superlative performance that is superior to the conventional PQ theory [14]. It has additional terms representing the oscillatory components in both active and reactive power. The final expression of powers using the extended PQ theory contains the positive and negative sequence components of the source voltage vector as well as the source current vector. Estimating sequence components is a tedious task that involves multiple numbers of SOGIs that form an interconnected structure [15], [16]. This high complexity in the power estimation process has not been adequately addressed in previous works.

In view of this, to bridge the gap, this article proposes

Manuscript received on May 6, 2024; revised on September 3, 2024; accepted on September 23, 2024. This paper was recommended by Associate Editor Chainarin Ekkaravarodome.

[1]The author is with Centurion University of Technology and Management, Odisha.

[2]The author is with Biju Patnaik University of Technology, Rourkela, Odisha.

[3]The author is with Shri Mata Vaishno Devi University Katra, India.

[4]The author is with Indira Gandhi Institute of Technology, Sarang.

[5]The author is with Odisha University of Technology, and Research, Bhubaneswar, Odisha.

[†]Corresponding author: satyanarayan.padhy@gmail.com

Digital Object Identifier: 10.37936/ecti-eec.2525231.253979

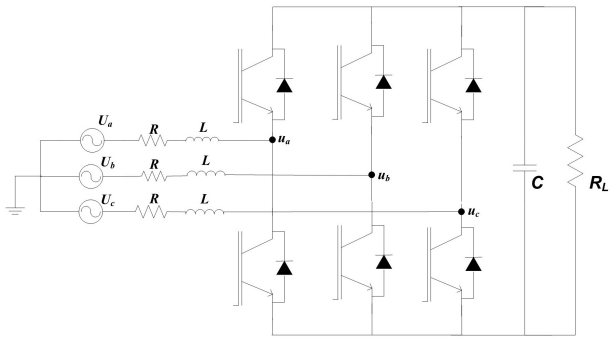

***Fig. 1**: The circuit of the converter.*

to use a distinct and novel approach by utilizing ANN models for the estimation of instantaneous active and reactive power instead of the complex structures that use a number of SOGIs. ANN, in combination with parallel processing, certainly promises to reduce the complexity. Hence this research article introduces a significant contribution to the field of rectifier control in unbalanced three-phase power systems at the industrial consumer level. The prevalent issue of control challenges with PWM rectifiers in such scenarios is addressed by proposing a novel approach that employs Artificial Neural Networks (ANN) for instantaneous power estimation. Unlike traditional methods involving complex structures with back-to-back connected Second Order Generalized Integrator (SOGI) blocks, the proposed method utilizes ANN to simplify the system, overcoming computational complexity challenges. The article demonstrates through rigorous simulations in MATLAB Simulink and the real-time simulation using the OPAL-RT environment that the ANN-based approach not only replicates the performance of SOGI-based systems but also significantly reduces the computational burden. This breakthrough leads to improved real-time response in unbalanced grid conditions, showcasing the potential of the proposed method for enhancing the control efficiency of PWM rectifiers in industrial applications.

2. SYSTEM MODEL

The common way of integrating the dc load to the ac grid is the ac-dc converter, whose circuit is given in the Fig. 1.

Considering U and i as the source voltage and current vectors, the above circuit system equation can be represented as (1), whose derivation is given in countless articles [3], [17], and [18] in the literature. The symbols p and q represent the instantaneous active and reactive powers, respectively. On the left-hand side, the gradients of these quantities are given.

$$\begin{aligned} \Delta\dot{p} &= \frac{1}{L}[|U| - Re(u * U)] - \omega q \\ \Delta\dot{q} &= -\frac{1.5}{L} Im(u * U) + \omega q \end{aligned} \tag{1}$$

Extended PQ theory presents a new definition of the instantaneous powers, which takes the scalar form, as shown in (2) [14].

$$\begin{bmatrix} p \\ q \end{bmatrix} = \begin{bmatrix} P_1 + P_2\cos 2\omega t + P_3 \sin 2\omega t \\ Q_1 + Q_2 \cos 2\omega t + Q_3 \sin 2\omega t \end{bmatrix}, \tag{2}$$

where,

$$\begin{cases} P_{dc} = \frac{3}{2}(i^+_{\alpha\beta} \cdot U^+_{\alpha\beta} + i^-_{\alpha\beta} \cdot U^-_{\alpha\beta}) \\ Q_{dc} = \frac{3}{2}(i^+_{\alpha\beta} \times U^+_{\alpha\beta} - i^-_{\alpha\beta} \times U^-_{\alpha\beta}) \\ P_{\cos} = \frac{3}{2}(i^+_{\alpha\beta} \cdot U^-_{\alpha\beta} + i^-_{\alpha\beta} \cdot U^+_{\alpha\beta}) \\ P_{\sin} = \frac{3}{2}(i^+_{\alpha\beta} \times U^+_{\alpha\beta} - i^-_{\alpha\beta} \times U^+_{\alpha\beta}) \\ Q_{\cos} = \frac{3}{2}(i^-_{\alpha\beta} \times U^+_{\alpha\beta} - i^+_{\alpha\beta} \times U^+_{\alpha\beta}) = -P_{\sin} \\ Q_{\sin} = \frac{3}{2}(i^+_{\alpha\beta} \cdot U^-_{\alpha\beta} + i^-_{\alpha\beta} \cdot U^+_{\alpha\beta}) = P_{\cos} \end{cases}$$

It includes the sequence components of the source voltage and current vector. In order to evaluate the PSC of any of the vectors, 2 SOGIs are required.

Modelling of SOGI

A block diagram showing the estimation for the PSC is shown in Fig. 2 [15], [19]. The ability of SOGI-QSG is to provide filtering capabilities beyond the conventional filters, which makes it flexible in handling the complex conditions of the grid. Here, the SOGI-QSG is used to estimate the positive-sequence component (PSC) in challenging grid conditions characterized by a weak grid with unbalanced phase voltages, frequency variations, harmonic distortion, and voltage sags. The PSC represents the positive sequence voltage component of the three-phase grid voltage.

The estimation process involves two separate SOGI blocks, each dedicated to one component of the Clarke transform to estimate the PSC. The SOGI blocks enable the extraction of a positive sequence from the three-phase voltage. Consequently, the positive sequence calculator processes the output from SOGI-QSGs to obtain positive sequence components $f_{\alpha+}$ and $f_{\beta+}$. Various studies have been conducted by researchers to compare and validate the performance of different SOGI-based models, which demonstrated that these models are highly effective and robust in improving the accuracy of PSC estimations and overall performance in grid synchronization under various grid conditions. Similarly, the same has to be followed for the source current vector. Again, estimating the negative sequence components requires additional SOGI blocks, as explained for the PSC. The transfer function of the SOGI-QSG model is a second-order filter and a phase shift to achieve an accurate estimation of phase. The typical transfer function of the model is given as (3).

$$\frac{k\omega_c^2}{s^2 + 2\xi\omega_c s + \omega_c^2}, \tag{3}$$

where k = Gain = $\sqrt{2}$, ζ = Damping Ratio = 0.75, and ω_c = Supply frequency.

The natural frequency ω_c determines the frequency at which the model responds to the input signal. The damping ratio ζ determines the stability and transient response of the model. The value of ζ is selected to

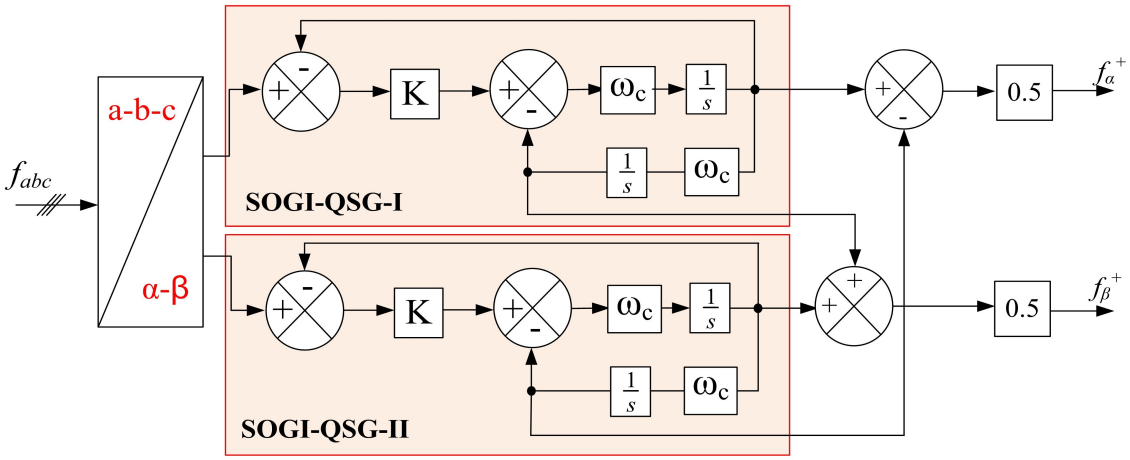

***Fig. 2**: Block representation of extraction of PSC.*

operate the system under critically damped conditions to offer a fast response without any overshoot.

3. SWITCHING ALGORITHM

Model Predictive Control (MPC) [20], [21] introduces a transformative paradigm in the realm of Direct Power Control (DPC) for PWM rectifiers at the industrial level. Unlike traditional methods, MPC optimally predicts future system behaviour and computes control actions accordingly, enhancing the rectifier's performance. In the context of DPC, MPC provides an advanced control strategy by systematically addressing unbalanced three-phase supply challenges. This approach optimizes power estimation, ensuring efficient utilization of the rectifier while mitigating control issues. By incorporating MPC into DPC, the system achieves superior real-time response, making it a promising advancement in the field of PWM rectifier control for industrial applications. The values of the control variables at the upcoming sampling instant are estimated using the system model and Euler's theorem. This is mathematically represented as (4). The relationship shown in (1) will be used here to calculate the predicted value [7], [22].

$$\left.\begin{aligned} p_{k+1} &= p_k + \Delta\dot{p}T_s \\ q_{k+1} &= q_k + \Delta\dot{q}T_s \end{aligned}\right\} \tag{4}$$

After that, the cost function shown in (5) is minimized to obtain the appropriate switching combination, which is to be fed to the converter module.

$$CF = \sqrt{(P_{ref} - p_{k+1})^2 + (Q_{ref} - q_{k+1})^2} \tag{5}$$

4. ARTIFICIAL NEURAL NETWORK (ANN)

The ANN, or the feed-forward neural network, plays a vital part in the power of electronic converters. These systems are often regarded as involved with highly complex non-linearities and dynamic behavior. ANN is capable of capturing these intricate relationships and, hence, can provide accurate modeling and control. Their adaptability allows for handling uncertainties and conditions where the load change occurs. They also provide the system with rapid responses to the changes in the system parameters. Additionally, the ANNs can learn from historical data that further improvements in the converter performance can be achieved.

4.1 Theory of ANN

This work emphasizes training the network on feed-forward neural networks, which are also said to be multilayer perceptron's (MLPs). In this type of ANN, the information flows in one direction through the layers, that is, in the forward direction, starting from the input layer to the output layer. Each layer consists of nodes or neurons. Each connection between nodes has a weight associated with it. The output of the node is calculated by applying an activation function to all the weighted sum of the inputs [23].

Consider X as the input vector, $W^{(l)}$ denotes the weight matrix of the l^{th} layer, $b^{(l)}$ represents the bias matrix, and $A^{(l)}$ is the activation at layer l. Here, Z refers to the linear transformation at the layer, while f is the activation function for the corresponding layer. The forward pass equation for the input layer is shown in (6).

$$A^{(0)} = X \tag{6}$$

The forward pass equation for the hidden layers is shown in (7).

$$\begin{aligned} Z^{(l)} &= W^{(l)}A^{(l-1)} + b^{(l)} \\ A^{(l)} &= f^{(l)}(Z^{(l)}) \end{aligned} \tag{7}$$

Here, l denotes the layer index.

For a network having L layers, the output of the last layer is the final prediction of the network, whose expression can be given as (8).

$$\hat{Y} = A^{(L)} \tag{8}$$

Training an FNN is essentially adjusting weights and biases to get the minimum difference between the

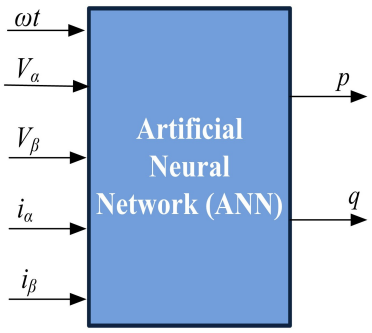

***Fig. 3**: The ANN base power estimation in blocks.*

predicted value of the network and the desired result. This is achieved by backpropagation, which calculates the error gradient with respect to each weight and bias. In an iterative process, the weights and biases are updated in a way that reduces error. Mathematically, a cost function J is minimized with respect to the actual labels Y.

One of the founding stones of the FNN is the universal approximation theorem. It states that a single hidden layer with enough neurons can approximate any continuous function accurately if appropriate training data and activation functions are used.

4.2 Training of the ANN

Dataset Generation

The dataset was developed by running simulations in MATLAB/Simulink for a variety of operating conditions representative of three-phase power unbalanced systems. The dataset contains 60,000 samples, which gives the basis necessary to cover a wide spectrum of scenarios, including voltage and current imbalance variations.

Architecture

This large dataset has five input features and two outputs. The five inputs are the stationary components of the source voltage and current vectors, along with their phase angle. While the instantaneous active and reactive powers are the outputs of the desired ANN. The architecture also includes hidden layers where it houses 7 neurons. More is the number of neurons, the more is the complexity, so it is restricted to 7. As the output layer has two variables, the network can predict both parameters simultaneously. The inputs and outputs of the designed ANN are represented in block, as shown in Fig. 3.

Training

In this work, the ANN was trained with improved optimization methodologies to make its learning efficient and strong. The Levenberg-Marquardt training algorithm is employed to train the network for its well-known advantage of high efficiency in minimizing errors and providing accelerated convergence. The hidden layers utilized the hyperbolic tangent sigmoid transfer function, which effectively introduces non-linearity, enabling the network to capture intricate patterns and relationships

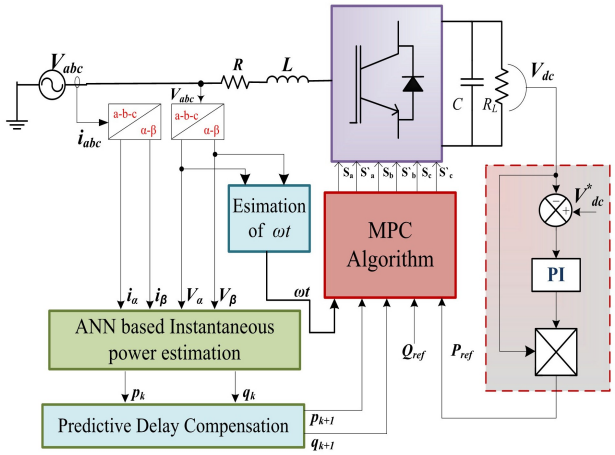

***Fig. 4**: Block diagram of the system.*

within the data. The output layer used a linear activation function for regression problems to allow the continuous values to be predicted. In contrast, a logistic sigmoid activation function was used with classification problems to map outputs to a probabilistic range between 0 and 1.

Weights and biases were initialized through the Nguyen-Widrow method. This is a strategy aimed at making the training process faster and more stable by starting with optimal initial values. During training, the performance of the network has been checked strictly by the mean squared error (MSE) metric, which quantifies the discrepancy between the predicted outputs and real target values, hence guiding the optimization process. Throughout the training process, the ANN adjusts the weights and biases to minimize the MSE. The value of MSE is a crucial metric to judge the correctness of the trained model by evaluating the difference between the predicted value and the real value. After training, validation is performed to monitor the accuracy. Last but not least, the test set permits independent assessment of the predictive abilities of a trained network, hence assuring it will be both robust and applicable within the real world. The complete system is in a block, as shown in Fig 4.

5. REAL-TIME SIMULATION

Digital simulations use a computer to evaluate mathematical functions and equations in a system model. Real-time simulation matches the pace of the real world, while offline simulation waits for the result of each step before proceeding. Overrun occurs in real-time simulation if the system model cannot be evaluated within the stipulated time step. Overrun-free simulation confirms that the processor can handle all computations within time constraints, ensuring reliable performance when implemented physically. However, offline simulation does not consider overrun, leading to operational limitations when implemented practically. Thus, from the offline simulation, the feasibility cannot be guaranteed completely. For real-time implementation, the OP5142

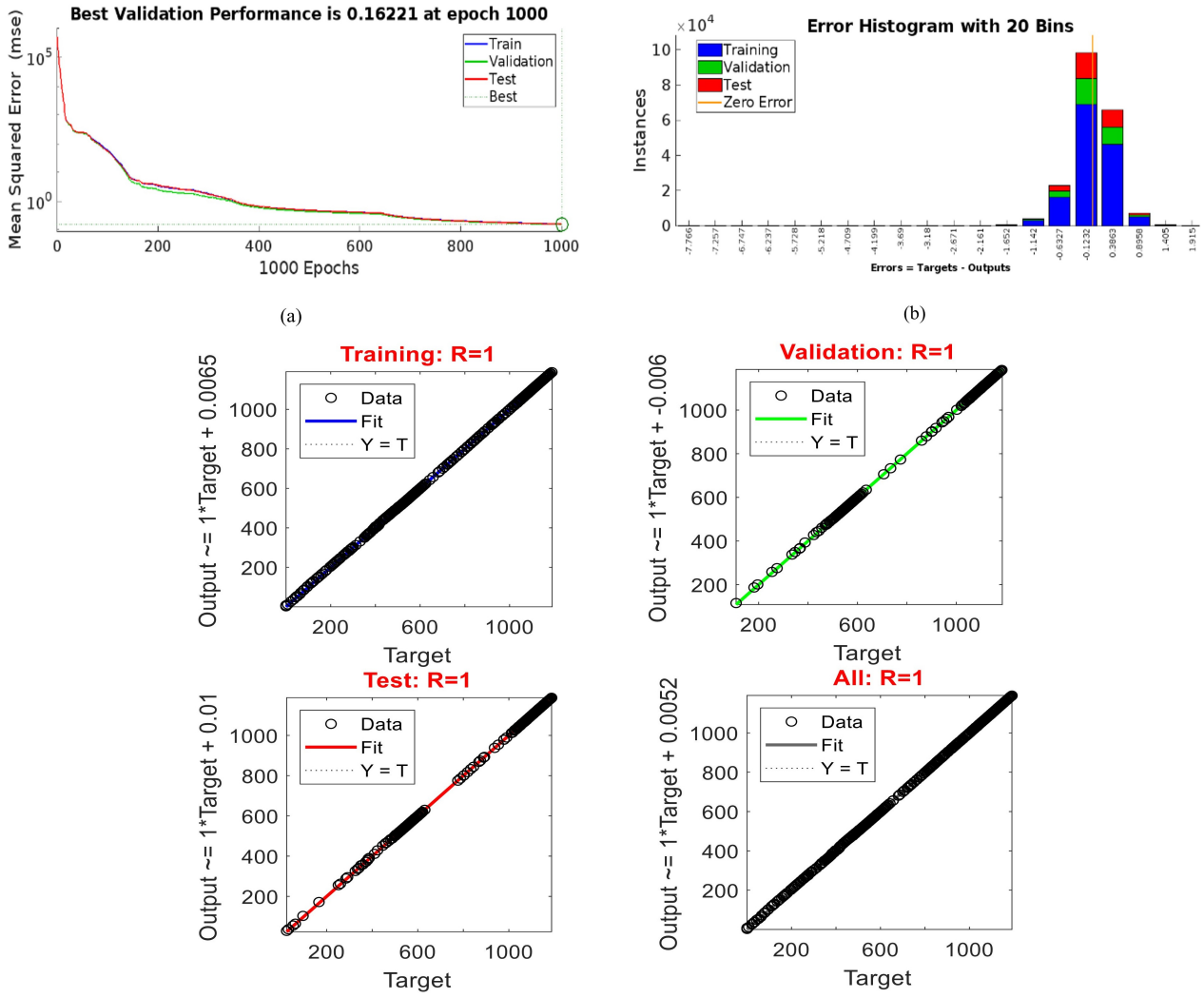

***Fig. 5**: Curves showing accurate ANN training (a) MSE (b) Error histogram (c) Regression curves.*

digital simulator from OPAL-RT Technologies is used as the controller, which is equipped with a 2.40 GHz Intel Xeon quad-core processor. The Host PC is connected to the OP-5142 Digital Simulator via a PCIe interface. The OP-5142 serves as a reconfigurable platform for real-time digital simulation. The computational burden on the processor can be evaluated from the execution time determined by the in-built OP-Monitor block of the RT-Lab environment. The op monitor block measures various timing information about the model.

***Table 1**: Simulation Parameter.*

Symbols	Description	System Parameters
V_{abc}	Three-phase supply	60 V
V_{dc}^{*}	Desired dc voltage	180 V
C	DC-bus capacitance	2000 μF
R	Line Resistance	0.6 Ω
R_L	Load	30 Ω
L	Line Inductance	12 mH
t_s	Sampling time	50 ms

6. RESULTS AND DISCUSSIONS

Rigorous simulation studies have been performed on MATLAB/Simulink, followed by its real-time evaluation on the RT-Lab platform to test the proposed system. The performance of the proposed are evaluated under different grid conditions as given in the IEEE standard-519 [24]. The values of the system parameters taken in the system are tabulated in Table 1. All the circuit parameters and the other model parameters are kept the same while testing the conventional SOGI-based system and the proposed ANN-based prediction of the instantaneous powers. After training the network, a Simulink block of the trained network is built. This is directly used in the MATLAB model of the system. Different training parameters are shown in Fig. 6, which generally aims to demonstrate the accuracy of the ANN model. The analysis of the parameters is given in the

subsequent paragraph.

The Levenberg-Marquardt training algorithm was employed to train an Artificial Neural Network (ANN) with 1000 iterations, resulting in a final Mean Squared Error (MSE) of 0.16221. A lower MSE indicates greater model accuracy. In this case, the final MSE of 0.16221 suggests that the ANN has achieved a reasonably low level of error in approximating the target values during the training process. The convergence of the algorithm over 1000 iterations is indicative of its effectiveness in minimizing the error and optimizing the network's weights and biases.

Insights and Analysis of the Trained ANN Model

The error histogram diagram is useful for analyzing ANN performance during training. The error histogram for the ANN training in this work is given in Fig. 5 (b). It provides information regarding the distribution of errors between target values and predicted outputs by the ANN. There are 20 bins representing ranges of error values in this histogram. These error values—Targets-Outputs—run on the x-axis from -0.15 to 0.15. The y-axis measures the frequency of the cases falling within each error bin. If the "Zero Error" stack is tall, that simply means a lot of instances have near-zero absolute errors, so they are very well fitted. All other non-zero errors in other bins are the discrepancies between targets and outputs for different phases: train, validation, and test. Overfitting or underfitting is identified by the spread of errors across bins. Fig. 5 (b) shows a tall stack at the "Zero Error" bin, indicating that a significant number of instances have errors close to zero, suggesting good performance.

The diagram shown in Fig. 5 (c) consists of four scatter plots, each representing a different dataset: Training, Test, Validation, and All. These plots visually demonstrate how well the model's predictions align with the actual target values. In each plot, data points are represented as circles, and there's a diagonal line (the "fit" line) that represents the ideal relationship between the predicted output and the actual target value. Furthermore, the stated final regression value 1 suggests a strong linear connection between projected and actual values. A regression result of one indicates that the model perfectly reflects the underlying patterns in the training data. This strong regression score underlines the ANN's predictability. It shows that the selected Levenberg-Marquardt training procedure effectively navigated the optimization landscape to arrive at a model that generalizes well to previously unknown data. The combination of a low MSE and a regression score of 1 demonstrates the trained ANN's resilience and efficacy in capturing complicated patterns in the dataset.

The steady-state performance of the PWM rectifier is analyzed from the waveforms presented in Fig 6 and Fig 7, which show the source voltage, current, and powers in the respective order.

From Fig 6, it can be observed that the supply voltage remains balanced until 0.5 s, and beyond that, a single phase voltage dip is introduced by decreasing phase a to 75%. Similarly, in Fig. 7, the RTS results for single-phase voltage rise and distorted voltage are shown. Initially, the grid supply voltage is programmed to have a single-phase voltage rise by raising the phase- 'a' voltage to 125%. Close observation of Figs. 6 and 7 reveals that they are pretty similar to each other, emphasizing the finding that the trained network is able to do its job perfectly by estimating the active and reactive powers accurately as per the extended power theory.

From Fig. 8, it can be observed that both SOGI and ANN estimations follow similar trends in the time interval while tracking each other closely, especially in the steady state periods.

It can be seen that the two methods align well, first in the lower power regions, say between 400 W and 800 W, and again in the higher power regions at around 1200 W. This confirms that the estimation of power by both methods is good within these ranges.

From Fig. 9, both the SOGI and ANN estimates track very well, as the trends in both these estimation methods are similar throughout the time interval. This would tend to indicate that both methods are effective estimators of reactive power within this range. After the initial transient has settled after about 0.05 seconds, both methods have a similar level of oscillation around the zero reactive power level.

The performance parameters, such as source current THD and ripple contents in p and q for the balanced grid, unbalanced grid, and distorted grid of the proposed controller (ANN-MPC), along with existing conventional

***Table 2**: Obtained Performance Parameters with Unbalanced Grid.*

Method	$THD(\%)$	$P_{RIP}(W)$	$Q_{RIP}(VAr)$
C-MPC [14]	2.02	19.3	14.9
LC-MPC [9]	2.03	19.3	14.9
ANN-MPC (Proposed)	2.01	19.3	14.9

***Table 3**: Obtained Performance Parameters with Unbalanced Grid.*

Method	$THD(\%)$	$P_{RIP}(W)$	$Q_{RIP}(VAr)$
C-MPC [14]	2.68	21.2	15.5
LC-MPC [9]	2.70	21.2	15.5
ANN-MPC (Proposed)	2.70	21.2	15.5

***Table 4**: Obtained Performance Parameters with Unbalanced Grid.*

Method	$THD(\%)$	$P_{RIP}(W)$	$Q_{RIP}(VAr)$
C-MPC [14]	2.23	19.8	15.1
LC-MPC [9]	2.24	19.8	15.1
ANN-MPC (Proposed)	2.25	19.8	15.1

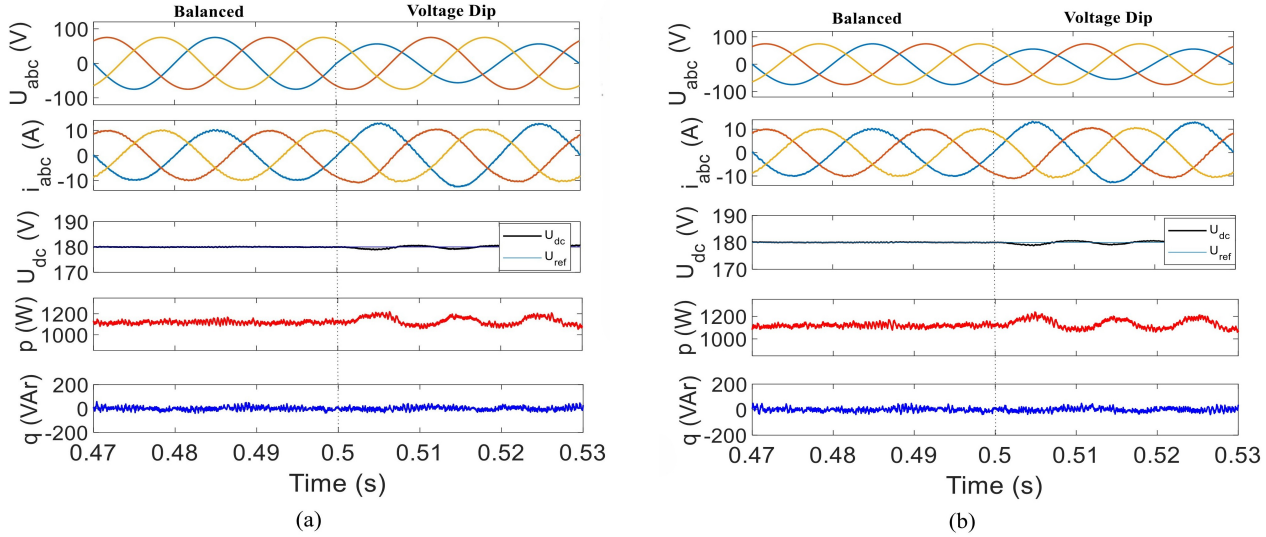

***Fig. 6**: RTS results of the converter for grid with balanced voltage and single phase voltage dip (a) with conventional SOGIs and (b) With ANN.*

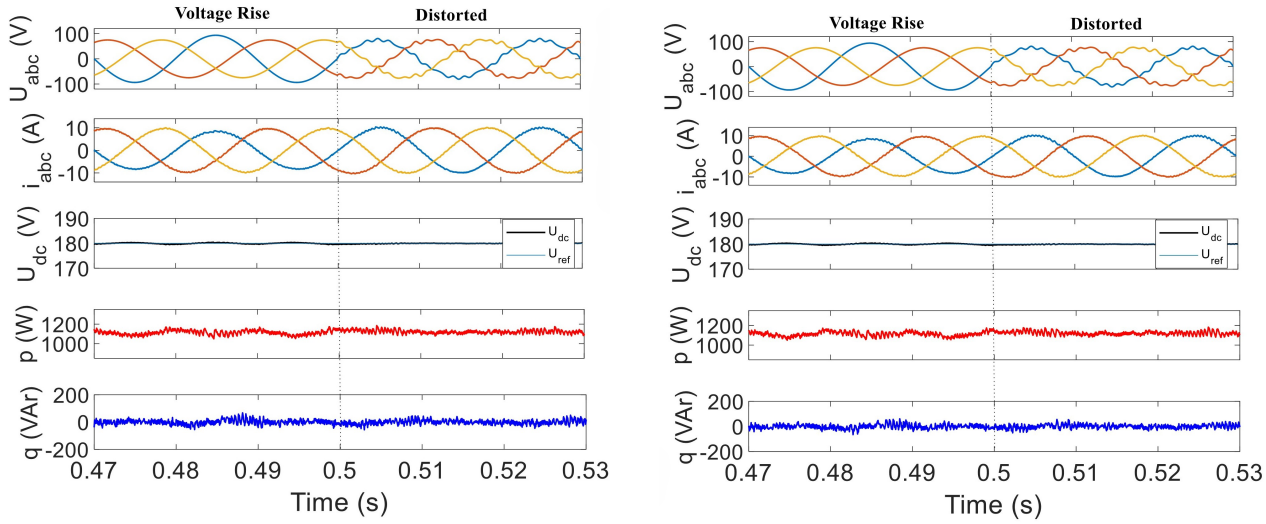

***Fig. 7**: RTS results of the converter for single phase voltage rise and distorted grid (a) with conventional SOGIs and (b) With ANN.*

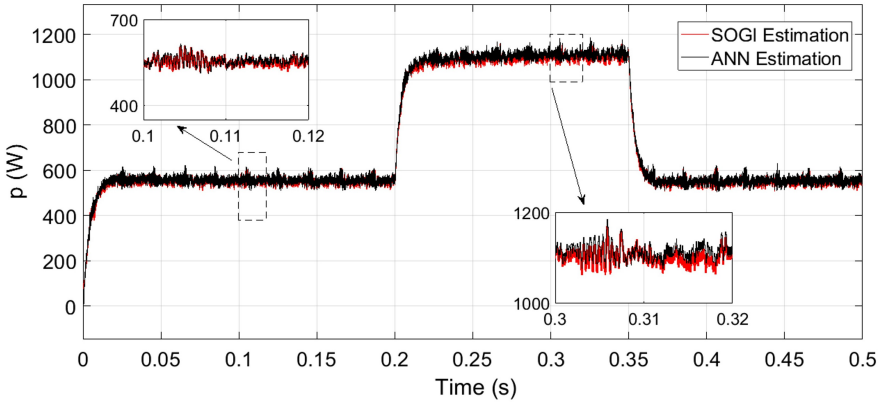

***Fig. 8**: Comparative result for active power estimation.*

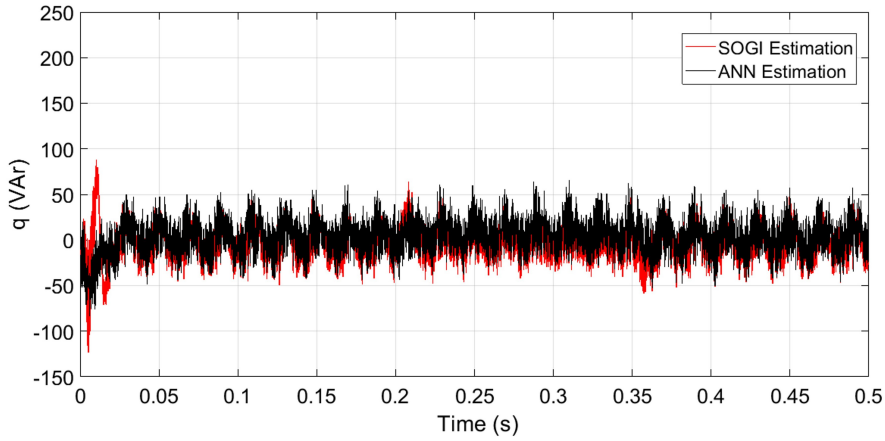

***Fig. 9**: Compartive result for reactive power estimation.*

MPC (C-MPC) and low-complexity MPC (LC-MPC), are tabulated in Table 2, Table 3, and Table 4, respectively. The power ripples are evaluated as per the methods given in the literature [17]. It can be observed that the values of the THD, Prip, and Qrip for all three methods are almost identical. Hence it can be safely concluded that the proposed method is able to replicate the performances obtained by established controllers [9], [14].

The computational complexity of both the conventional control and the proposed ANN-based power estimation are compared in the RT-Lab environment. It was found that the mean execution time for C-MPC is 10.11 µs, while the proposed method brings it down to 8.34 µs. This proves that there has been a reduction in computational complexity of around 16%. On the other hand, the LC-MPC operates with an average execution time of 6.80 µs, giving rise to a 32.7% reduction in computational burden. However, with LC-MPC [9], it is impossible to add additional non-linear constraints to the cost function as facilitated by the C-MPC [14] and the proposed ANN-MPC.

7. CONCLUSION

This paper presents an innovative approach to managing PWM rectifiers in the presence of unbalanced three-phase power sources at the industrial consumer. In unbalanced grids, the typical direct power control (DPC) technique, which is based on active and reactive power estimations, confronts complexity, necessitating the usage of extended *pq* theory. This paper argues for the use of ANN as a potential alternative to complicated architectures based on back-to-back coupled SOGIs. The results show that ANN offers an adaptable solution circumventing the complexities associated with the traditional interconnected SOGI structures. The adaptability and learning capabilities of the ANN make it an attractive choice for applications requiring a wide range of active power operations. Looking at the immense potential yet to be explored, the researchers embrace the paradigm shift of adopting ANN in power electronic converters. Real-time simulations in RT-LAB validate the accuracy of the proposed method.

REFERENCES

[1] Y. Zhang and C. Qu, "Direct Power Control of a Pulse Width Modulation Rectifier Using Space Vector Modulation Under Unbalanced Grid Voltages," *IEEE Trans. Power Electron.*, vol. 30, no. 10, pp. 5892–5901, 2015, doi: 10.1109/TPEL.2014.2371469.

[2] P. Antoniewicz and M. P. Kazmierkowski, "Virtual-flux-based predictive direct power control of AC/DC converters with online inductance estimation," *IEEE Trans. Ind. Electron.*, vol. 55, no. 12, pp. 4381–4390, 2008, doi: 10.1109/TIE.2008.2007519.

[3] A. Rath and G. Srungavarapu, "New Model Predictive & Algorithm DPC based Shunt Active Power Filters (SAPFs)," in *2021 1st International Conference on Power Electronics and Energy (ICPEE), IEEE*, Jan. 2021, pp. 1–6. doi: 10.1109/ICPEE50452.2021.9358550.

[4] A. Rath and G. Srungavarapu, "Delay Compensated Multifold Table (DCMST) Direct Power Control (DPC) with Duty Ratio Control," in *2022 4th International Conference on Energy, Power and Environment (ICEPE), IEEE*, Apr. 2022, pp. 1–6. doi: 10.1109/ICEPE55035.2022.9798177.

[5] A. Rath and G. Srungavarapu, "Reduced complexity model predictive direct power control for unbalanced grid," *Electr. Power Syst. Res.*, vol. 234, p. 110563, Sep. 2024, doi: 10.1016/j.epsr.2024.110563.

[6] A. Rath and G. Srungavarapu, "Battery Charging With Model Predictive DPC based-Converter Using Dynamic DC-link Reference," in *2022 4th International Conference on Energy, Power and Environment (ICEPE), IEEE*, Apr. 2022, pp. 1–6. doi: 10.1109/ICEPE55035.2022.9797948.

[7] J. Hu, J. Zhu, G. Lei, G. Platt, and D. G. Dorrell, "Multi-objective model-predictive control for high-power converters," *IEEE Trans. Energy*

Convers., vol. 28, no. 3, pp. 652–663, 2013, doi: 10.1109/TEC.2013.2270557.

[8] Y. Zhang, Z. Li, Y. Zhang, W. Xie, Z. Piao, and C. Hu, "Performance improvement of direct power control of pwm rectifier with simple calculation," *IEEE Trans. Power Electron.*, vol. 28, no. 7, pp. 3428–3437, 2013, doi: 10.1109/TPEL.2012.2222050.

[9] Y. Zhang and W. Xie, "Low complexity model predictive control - Single vector-based approach," *IEEE Trans. Power Electron.*, vol. 29, no. 10, pp. 5532–5541, 2014, doi: 10.1109/TPEL.2013.2291005.

[10] Y. Zhang, W. Xie, Z. Li, and Y. Zhang, "Low-complexity model predictive power control: Double-vector-based approach," *IEEE Trans. Ind. Electron.*, vol. 61, no. 11, pp. 5871–5880, 2014, doi: 10.1109/TIE.2014.2304935.

[11] D. Wang et al., "Model Predictive Control Using Artificial Neural Network for Power Converters," *IEEE Trans. Ind. Electron.*, vol. 69, no. 4, pp. 3689–3699, Apr. 2022, doi: 10.1109/TIE.2021.3076721.

[12] P. Vu, B. B. Pho, H. M. Tran, and M. T. Tran, "An artificial neural network-based model predictive control of cascaded h-bridge multilevel inverter," *Int. J. Renew. Energy Res.*, vol. 12, no. 3, 2022, doi: 10.20508/ijrer.v12i3.13145.g8513.

[13] H. Acikgoz, A. Kumar, H. Beiranvand, and M. Sekkeli, "Hardware implementation of type-2 neuro-fuzzy controller-based direct power control for three-phase active front-end rectifiers," *Int. Trans. Electr. Energy Syst.*, vol. 29, no. 10, pp. 1–14, 2019, doi: 10.1002/2050-7038.12066.

[14] Y. Zhang and C. Qu, "Model predictive direct power control of PWM rectifiers under unbalanced network conditions," *IEEE Trans. Ind. Electron.*, vol. 62, no. 7, pp. 4011–4022, 2015, doi: 10.1109/TIE.2014.2387796.

[15] A. Rath and G. Srungavarapu, "An Advanced Shunt Active Power Filter (SAPF) for Non-ideal Grid Using Predictive DPC," *IETE Tech. Rev.*, pp. 1–14, Oct. 2022, doi: 10.1080/02564602.2022.2127946.

[16] A. Rath and G. Srungavarapu, "Dead Beat Predictive DPC based Battery Charging System Using Dynamic DC-link Reference," in *2021 National Power Electronics Conference (NPEC), IEEE*, Dec. 2021, pp. 01–06. doi: 10.1109/NPEC52100.2021.9672500.

[17] A. Rath, A. Kumar, G. Srungavarapu, and M. Pattnaik, "Power quality improvement using 18 sector algorithm based direct power control," *Int. Trans. Electr. Energy Syst.*, vol. 31, no. 10, pp. 1–17, Oct. 2021, doi: 10.1002/2050-7038.12784.

[18] P. Cortés, J. Rodríguez, P. Antoniewicz, and M. Kazmierkowski, "Direct power control of an AFE using predictive control," *IEEE Trans. Power Electron.*, vol. 23, no. 5, pp. 2516–2523, 2008, doi: 10.1109/TPEL.2008.2002065.

[19] S. A. Nejad, J. Matas, J. Elmariachet, H. Martín, and J. de la Hoz, "Sogi-fll grid frequency monitoring with an error-based algorithm for a better response in face of voltage sag and swell faults," *Electron.*, vol. 10, no. 12, pp. 23–26, 2021, doi: 10.3390/electronics10121414.

[20] H. Fang, Z. Zhang, X. Feng, and R. Kennel, "Ripple-reduced model predictive direct power control for active front-end power converters with extended switching vectors and time-optimised control," *IET Power Electron.*, vol. 9, no. 9, pp. 1914–1923, 2016, doi: 10.1049/iet-pel.2015.0857.

[21] Y. Zhang, Y. Peng, and C. Qu, "Model Predictive Control and Direct Power Control for PWM Rectifiers with Active Power Ripple Minimization," *IEEE Trans. Ind. Appl.*, vol. 52, no. 6, pp. 4909–4918, 2016, doi: 10.1109/TIA.2016.2596240.

[22] Y. Zhang, Z. Wang, J. Jiao, and J. Liu, "Grid-Voltage Sensorless Model Predictive Control of Three-Phase PWM Rectifier under Unbalanced and Distorted Grid Voltages," *IEEE Trans. Power Electron.*, vol. 35, no. 8, pp. 8663–8672, 2020, doi: 10.1109/TPEL.2019.2963206.

[23] A. Rahoui, A. Bechouche, H. Seddiki, and D. Ould Abdeslam, "Virtual Flux Estimation for Sensorless Predictive Control of PWM Rectifiers under Unbalanced and Distorted Grid Conditions," *IEEE J. Emerg. Sel. Top. Power Electron.*, vol. 9, no. 2, pp. 1923–1937, 2021, doi: 10.1109/JESTPE.2020.2970042., pp. 652–663, 2013, doi: 10.1109/TEC.2013.2270557.

[24] D. Committee, I. Power, and E. Society, "IEEE 519 Recommended Practice and Requirements for Harmonic Control in Electric Power Systems IEEE Power and Energy Society," vol. 2014, 2014.

Abinash Rath received his B. Tech in Electrical Engineering from the Government College of Engineering Keonjhar, India, and his M. Tech in Power Electronics Control and Drives from VSSUT, Burla, India. He has completed his Ph.D. from the Department of Electrical Engineering, National Institute of Technology Rourkela, India. He is currently working as an Assistant professor in dept. of Electrical and Electronics Engineering at Centurion University of Technology and Management, Odisha. His research interests include power electronic converters, shunt active power filters, and power quality.

Satyanarayn Padhy received his B.Tech degree in Applied Electronics and Instrumentation Engineering from Biju Patnaik University of Technology in 2007 and an M.Tech in Electrical Engineering (Control & Instrumentation) from Motilal Nehru National Institute of Technology in 2013. He is currently pursuing Ph.D. at Biju Patnaik University of Technology, Rourkela, and also a Faculty Member at Centurion University of Technology and Management and currently working as an Assistant Professor in the Department of Electronics and Communication Engineering. His research interests are focused on DC-DC converters, controller design for power converters, ASIC Design, and analog & digital integrated circuit design.

Ankireddy Narendra has received a B.Tech degree in electrical and electronics engineering from Jawaharlal Nehru Technological University, Kakinada, India, in 2011, an M.E degree in power systems and automation from Andhra University, Visakhapatnam, in 2014 and has received his Ph.D in 2023 at the National Institute of Technology Rourkela, in the area of photovoltaics and machine drives. His area of research is solar photovoltaics, power electronic converters, electrical machine drives and dual active bridge DC-DC converters.

Ashutosh Biswal received his BTech degree in electrical engineering from Gandhi Institute of Science and Technology, Rayagada, Odisha, India in 2012 and MTech degree in power electronics control and drives from Veer Surendra Sai University of Technology, Burla, Odisha, India in 2015. He is currently pursuing PhD at the Department of electrical engineering, National Institute of Technology, Uttarakhand, India. His areas of interest are nonlinear control systems, artificial intelligence and automatic load frequency control.

Kanhu Charan Bhuyan received his B.Tech. degree in Electronics and Instrumentation Engineering from the College of Engineering and Technology (affiliated to Biju Patnaik University of Technology), Odisha, India in 2003, and his M.Tech. degree in Control and Automation specialization from IIT, Delhi, India in 2005. He received his Ph.D. degree from NIT, Rourkela, India in 2014. He works as an Associate Professor at the Electronics and Instrumentation department, Odisha University of Technology and Research, Bhubaneswar. His current research interests include digital VLSI, IoT, modeling of photovoltaic cells, fuel cells, and control strategies of various power converter and renewable power generation systems.